

Synergy of experiments and computer simulations in research of turbulent convection

K. Hanjalić *

Department of Multi-scale Physics, Delft University of Technology, Lorentzweg 1, Delft 2628 CJ, The Netherlands

Available online 10 November 2005

Abstract

We discuss the potential and limitations of current experimental and simulation techniques and their synergy in the research of turbulent convection. Examples from our recent experience are presented where complementing of experimental and simulation approaches has not only provided precious information, but has also revealed some unexpected phenomena which could have remained hidden if the problem was investigated only experimentally or only by simulations. Among examples considered are the two paradigms of turbulent flows and heat transfer, and a challenging MHD problem: 1. Thermal convection over horizontal surfaces in a broad range of conditions including extreme ones, covering experiments for $Ra = 10^8$ – 10^9 , DNS for $Ra = 10^5$ – 10^8 , LES for 10^6 – 10^9 and VLES/T-RANS for $Ra = 10^6$ – 2×10^{16} ; 2. Experimental, RANS and LES studies of flow structure and heat transfer in single and multiple impinging jets at higher Re numbers; 3. Computer-simulation of a model of fluid-magnetic dynamo, in association with experiments in Riga (Latvia) and Dresden (Germany).

© 2005 Elsevier Inc. All rights reserved.

Keywords: Turbulent convection; Experiments; Computer simulations; Synergy

1. Introduction

Benefits of synergy of experiments, theories, analytical, computational and other research methods, have long been recognized in science and all methods have been practiced in parallel, complementing each other. Yet, scientists tend to specialize in one or other research method or field, remaining predominantly either experimentalists, theoreticians, or numericists (computationalists). The research interaction often remains within relatively closed communities, results are published in specialized experimental, theoretical or computational journals, and communications practiced at specialized conferences.

A particular gap emerged with the advent and rapid development of computer simulations. These have been adored and worshiped by some to the point of exaltation ('experiments will become obsolete and wind tunnels will

be turned into computer output storages'), while mistrusted and undermined by others, sometimes to the point of ridicule ('garbage in, garbage out'). As we all know, wind tunnels were not converted into storages. Not because the computer printouts disappeared and gave way to electronic media and graphics, but because experimental research has been steadily gaining in importance, inspired and promoted—paradoxically or not—also by computer simulations. The development of simulation techniques requires (next to theory) reliable data for validating, verifying and calibrating numerical schemes, methods, mathematical models, and such data in most cases can be provided only by measurements. A large number of experiments have been dedicated specifically to provide reference data for validating models and methods used in simulations. The reverse is also true: most simulations, especially when promoting new methods or models, focus on problems already investigated experimentally, thus replicating experiments (often for its own sake to verify the theory or model and to provide a proof of accuracy) but producing more data and new information, some of which may be inaccessible

* Tel.: +31 15 278 1735; fax: +31 15 278 1204.

E-mail address: hanjalic@ws.tn.tudelft.nl

to experiments. It is this kind of mutual feedback between experimental and simulation research that has shown especially great potential for synergy.

The progress in laser and spectroscopic diagnostics (LDA, PIV, PTF, LIF, CARS, etc.), in holography, MRI and other new techniques, have opened new prospects for non-intrusive measurements of *almost* all relevant properties of flows, heat and mass transfer in non-reacting and reacting (combusting) single and multiphase flows. New wind tunnels have been built and more are planned, especially to achieve extreme Re and Ra numbers. In parallel, the techniques of computer simulations have made enormous progress making it possible, at least in a limited class of problems, to acquire *all* information required or imagined. The potential of computer simulations to provide full time-dependent three-dimensional fields has also prompted and stimulated spectacular progress in computer visualization and animation which make it possible to get a full insight into miniscule and subtle details of flow structures and their time evolution and dynamics in three-dimensional space.

Developing of *research methods* (experimental techniques and instruments, numerical schemes and models, specific theories, etc.) requires usually life dedication leaving little time and motivation for excursions into other areas and radical changes of research specialization. In contrast, research aimed at *acquiring new knowledge* and gaining deeper insight into physics of various phenomena can greatly benefit from combined and simultaneous experiments and computer simulations (with, of course, a blend of theory) in overcoming barriers and limitations of each, and expanding the frontiers of our cognition. A number of research groups are pursuing such a dual track.

The potential for synergy is broad and versatile; it is often unpredictable and sometimes comes as a surprise. In most cases one follows common sense by recognizing limitations and potentials of each method and compensates for deficiencies by using other methods. It is beyond the scope of this article to try to postulate rules and recommendations. Instead we present here some examples from our experience where complementing of experimental and simulation approaches has not only provided precious information, but has also revealed some unexpected phenomena which could have remained hidden if the problem was investigated only experimentally or only by simulations. Among examples considered are the two paradigms of turbulent flows and heat transfer, and a challenging MHD problem:

- Thermal convection over horizontal surfaces in a broad range of conditions including extreme ones: experiments for $Ra = 10^8$ – 10^9 , DNS for $Ra = 10^5$ – 10^8 , LES for 10^6 – 10^9 and VLES/T-RANS for $Ra = 10^6$ – 2×10^{16} .
- Impinging flows and heat transfer at higher Re numbers: experiments, RANS and LES of a single round jet for $Re = 20000$ $H/D = 2$ – 6 , and experiments and RANS of multiple jets in in-line and hexagonal arrangements.

- Computer-simulation of a model of fluid-magnetic dynamo, in association with experiments in Riga (Latvia) and Dresden (Germany).

2. Rayleigh–Bénard convection: Some old and new challenges

Rayleigh–Bénard (R–B) convection has long served as a paradigm of thermal convection. Despite its geometric simplicity – fluid trapped between two horizontal walls heated from below and cooled from above – at sufficiently high Rayleigh number $Ra = g\beta\Delta TL^3/\alpha\nu$ contains most events, structures and features pertinent to real large-scale phenomena in environmental, terrestrial and in many technological systems. Here β is the thermal expansion coefficient, α is temperature diffusivity, ν is kinematic viscosity, ΔT the imposed temperature difference and L the characteristic length scale.

Research in R–B convection has stirred much controversy. At the core is the $Nu \propto Ra^n$ correlation, where $Nu = hL/k$ is Nusselt number (where h is the heat transfer coefficient and k the fluid conductivity), but the scaling controversy reflects the general disagreement about the underlying physics and heat transfer mechanism. The interest, especially at high Ra ($>10^{12}$) is motivated not only by scientific curiosity, but also by the importance of the R–B phenomenon in understanding thermal convection in the atmosphere, oceans, earth mantle, and in engineering equipment.

The classic correlation $Nu = Ra^{1/3}$ implies no communication between the two horizontal walls (hence no effect of their distance) and the heat flux is assumed to be governed by the processes confined within the wall boundary layers. This implies that the plumes generated on one of the walls never reach the other wall. While this theory may sound reasonable at low Ra numbers, it seems unlikely at high Ra since persistent plumes (that may break into thermals or puffs) propelling and stretching from one to another wall have been observed experimentally as well as in numerical simulations. Wall communication involves a different heat transfer scenario, as argued by several researchers (e.g. Siggia, 1994) resulting in a different Ra exponent. Most evidence seems to support $2/7$ scaling (“hard” regime) observed by the Chicago group (Castaigne et al., 1989) for $Ra > 4 \times 10^7$ in their experiment with helium. However, other experiments using water report the $1/3$ power law for $Ra > 10^9$ with a smaller exponent for low Ra numbers (Siggia, 1994, p. 151). While the small difference in the Ra exponent may not be a reliable indicator, reports on other parameters, which provide better indication of the change in the regime, are also inconsistent.

Even larger controversy surrounds the very high Ra numbers, roughly beyond 10^{12} , for which the Grenoble group (Chavanne et al., 1997; Chavanne et al., 2001; Roche et al., 2001) observed another, “ultra hard” regime characterized by an increase in the Ra exponent to about 0.38 to 0.39 (for $10^{11} < Ra < 2 \times 10^{14}$), indicating a trend towards

the asymptotic value of 1/2 for infinite Ra numbers, postulated by Kraichnan (1962). They reported other anomalies in the ultimate regime such as a dramatic change in the spatial organization of temperature fluctuations, transition from the supposedly laminar to turbulent wall boundary layers, and a cross-over of the hydrodynamic (“velocity”) and thermal boundary layer thicknesses. The ultimate regime was earlier reported by the Chicago group (Wu, 1990) who found the Ra exponent to be as high as 0.49! Recently, Glazier et al. (1999), and Niemela (2000) disputed these finding on the basis of their experiments with mercury and helium, respectively.

Fig. 1 shows approximate ranges of Ra number corresponding to various regimes, as well as niches and limitations of experiments and various computational methods, over a 15-decade range of Ra number.

Apart from pioneering theories, the research in R–B convection has until recently been almost exclusively experimental, complemented with theories based usually on similarity and scaling arguments. Much has been learned, different regimes and phenomena discovered, but many questions still remain and new ones are being raised.

An illustrative example of a new/old challenge is the recent recording of irregular but sudden reversals of direction of wind velocity reported by Niemela et al. (2001) in their experiment with cryogenic helium in a cylindrical container of 50 cm in diameter and height, Fig. 2. The most

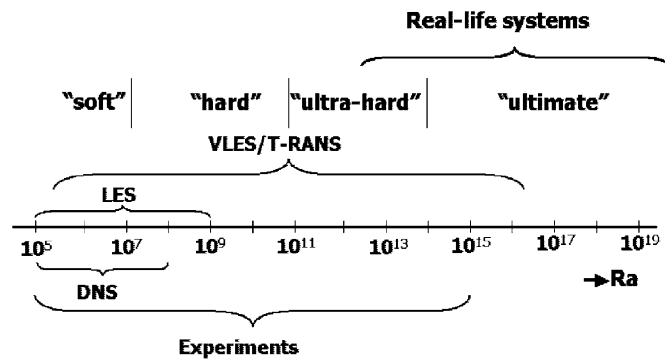


Fig. 1. Thermal convection: turbulence regimes and ranges of Ra number accessible to experimental and simulation methods.

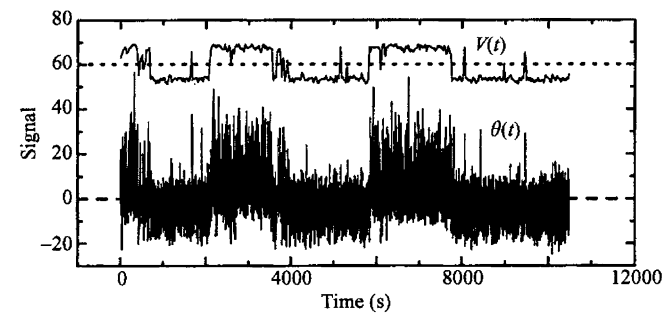


Fig. 2. Wind velocity (smoothed) and temperature recordings in experiment with cryogenic helium in a cylindrical enclosure 50×50 cm at $Ra = 1.5 \times 10^{11}$ (Niemela et al., 2001).

striking feature are the very long periods of sign reversal of $O(2000)$ sec of real time.

In contrast, in our pending experiment with water in a $60 \times 60 \times 15.5$ cm rectangular container at $Ra \approx 10^9$ we recorded also long-term periodic oscillations, but of a very different nature, with a smooth change of pattern with an average period of about 300–400 s, Fig. 3. The main difference, apart from Ra of two orders of magnitude (but still in the same regime of “hard turbulence”), is the aspect ratio, which hints to possible difference in large-scale convective cells and their dynamics.

Some, though still speculative explanation of the first phenomenon has been associated with the low aspect ratio, $O(1)$ of the Niemela et al. (2001) experiment (see further below), but the oscillations in the second example still await further experiments for possible clarification. True insight into this dynamics requires information about the complete velocity (and temperature) field, which is almost impossible to gather in experiment, especially at higher Ra numbers, as discussed below. Computer simulations if feasible could provide much more information about these

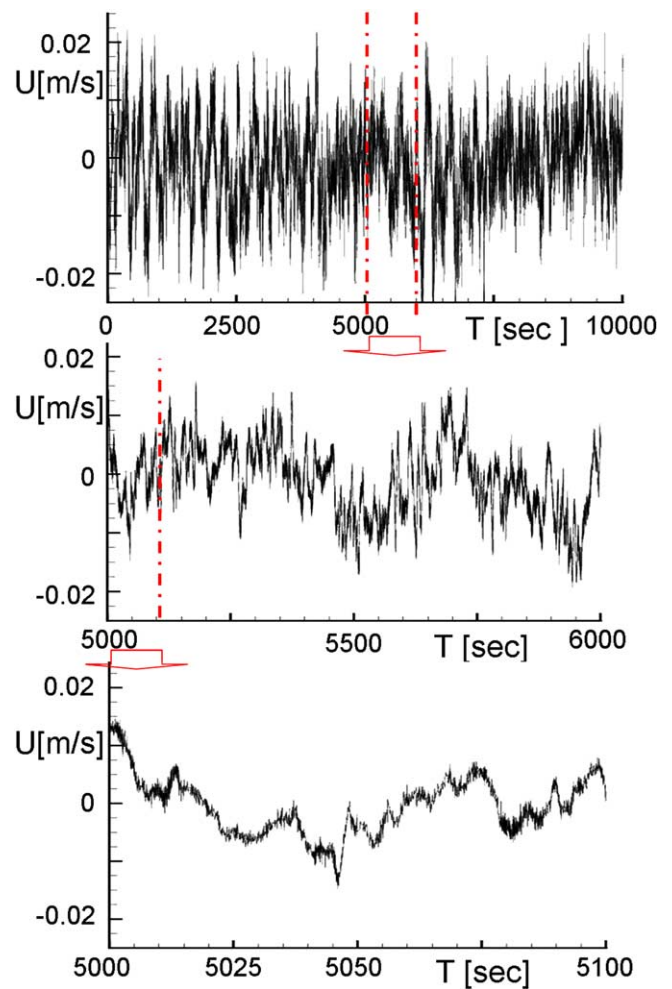


Fig. 3. LDA long-term velocity recording at 33 mm from the bottom wall in the center of a $60 \times 60 \times 15.5$ cm R–B experiment with water, $Ra \approx 10^9$ (Verdoold et al., in preparation).

events, but they also face serious limitations for high Ra numbers.

2.1. Limitations in R–B experiments

Let us first recall some major limitations and snares of experiment, with specific reference to R–B and similar problems. Until recently, experiments have primarily focused on point measurements of fluid temperature and velocity and wall temperature and heat flux, for which a number of interesting and ingenious methods have been reported (see e.g. Chavanne et al., 2001, for an overview of recent experiments). Only recently, with the development of PIV, PTF, LIF and suspended liquid crystals, field measurements have been made possible, but again only in one plane. Three-dimensional instantaneous and fluctuating fields, which are precious for capturing turbulence structures and its dynamics, are still beyond the full reach despite some promises of e.g. 3D and holographic PIV, or similar techniques. Simultaneous field measurements of velocity and temperature with e.g. PIV and suspended liquid crystals or CARS, which would provide information about the coupling of the two fields and their interaction (turbulent heat flux) are still at rudimentary stage of development, facing a number of problems related to mutual contamination of signals, different data rates of various techniques used (Tummers et al., 2004) and others. The problem becomes increasingly acute when aiming at higher Ra numbers, say beyond 10^{11} – 10^{12} (depending on the Prandtl number), corresponding to real situations of interest. The obvious parameter to increase is the height ($Ra \propto L^3$) of the experimental enclosure, but in order to keep a reasonable aspect ratio, the size of the rig increases dramatically beyond the limit of rational control of the experiment. The imposed temperature difference is usually limited for various reasons (control of experiment, strong inhomogeneity of fluid properties, non-Boussinesq effects). Choosing a fluid with low molecular transport coefficients α and ν remains thus the only rational way for achieving high Ra numbers. Among these, liquid helium at very low temperature, around its critical point (≈ 5 K), has been most popular making it possible to cover a wide range of Ra (by varying density using both gaseous and liquid helium) and to reach very high values of Ra up to 10^{16} (Chavanne et al., 2001; Niemela et al., 2001), and others. However, the use of liquid helium brings other problems related to control, and impairs the transparency and access to optical (especially field) measurements.

Another shortcoming of experiments in R–B convection is that they are all performed in enclosures, and most often of a small aspect ratio $A = W/H$ (width/height) of $O(1)$. However, the inevitability of side walls and the relatively low aspect ratio bring major limitation in imitating the infinite R–B convection, which corresponds more closely to the real problems of thermal convection encountered in nature. In a finite enclosure of $A = O(1)$ a circular motion (‘fly-wheel’) is self-generated over the whole enclosure in one

or other direction depending on initial inhomogeneities. As pointed above, every now and then the motion will reverse directions, exhibiting similar but mirrored pattern, Fig. 2 (Niemela et al., 2001). This self-organization, that can persist in a noisy environment, as well as dramatic excursions in one or other direction, are believed to occur also in large terrestrial systems, one example being associated also with the irregular reversal of Earth magnetic field. However, the irregularity (or the order, as the case may be) in an enclosure of a small aspect ratio and in large open (if not infinite) domains cannot be expected to have much in common, as shown in Fig. 3. In enclosures of large aspect ratio the organized large-scale convective circular motion tends to fill the whole space, especially at higher Ra numbers, but because of its length, it is less stable than in small aspect ratio cavities and it is likely to break into shorter cells with different directions and then coalesce again, which we believe is the source of oscillation displayed in Fig. 3.

The disagreements between different experimental findings have been found even in enclosures of the same or similar geometries. They can arise from differences in the experimental set-ups, size, geometry (rectangular–circular), difficulties in controlling the experiment (heat leakage) and from different width/height aspect ratios. Although the latter is claimed to have no effect for aspect ratios above 0.5, it is difficult to accept that the side walls, even if their thermal conditions are perfectly controlled, will not be influential through wall friction and blocking effects. Experimental evidence of convective rolls sweeping across the entire domain, confirmed by our simulations, with horizontal wave lengths expanding with an increase in Ra number if there is no side-wall blocking, is one of the indications of the side-wall effects. Observation at a single location, usually along the vertical line situated in the enclosure centre, may not be sufficient for drawing general conclusions about the flow structure in the entire domain.

2.2. Limitations in R–B computer simulation

Over the last decade or so, computer simulations (CS) of R–B convection have brought more information, making it possible to calculate properties and parameters that are still inaccessible to measurements. Moreover, the simulations have provided three-dimensional visualization and animations thus enabling full insight into structures and mechanisms. CS have also made possible to verify experimental findings, but have also been calibrated, validated and verified with respect to experiments, thus providing a very beneficial synergy. The question may arise: do we need both? Those engaged in simulations tend to claim that—provided that we are dealing with Ra numbers, geometries and fluid properties that are accessible to CS (for limitations see below)—CS are much more informative, and thus experiments could become redundant. But, as we all know, CS have some severe limitations on their own.

The most exact numerical approach to solving Navier–Stokes (N–S) equations is direct numerical simulation

(DNS) which resolves all scales up to the Kolmogorov ones. In order to make an estimation of possible attainable values of Ra at present, a simple analysis can be performed based on the ratio between the dissipation length scale and the distance between the horizontal walls, Kerr (1996): $\eta/H = 1/H(\nu^3/\varepsilon)^{1/4} = (Pr^2/(Nu - 1)Ra)^{1/4}$. By taking Niemela et al. (2001) experimental correlation, $Nu = 0.124Ra^{0.309}$, it is easy to show that in order to perform fully resolved calculations, one needs to apply 135, 33000 and 250000 grid points in the vertical direction for $Ra = 10^7$, 2×10^{14} , 10^{17} respectively. In addition, one has to take into account the time integration over sufficiently long periods (of at least a few convective time scales) and with sufficiently small time steps in order to resolve dissipative time scales. Meeting both the spatial and time resolution requirements puts at present the upper limit on the achievable Ra by DNS to approximately 10^9 , by using a massively parallelised computer. For example, a decade ago, for the DNS for $Ra = 2 \times 10^7$, Kerr (1996) used $256^2 \times 96$ grid points and required 400 h of CRAY-YMP to simulate just one convective time scale. Recently, Van Reeuwijk (in preparation) in our group moved up the frontier with new DNS of R–B convection for the record $Ra = 1.1 \times 10^8$ and for $Pr = 7$ in a $4 \times 4 \times 1$ enclosure using a $768^2 \times 320$ grid (close to 200 million cells!) clustered towards the walls, using a finite volume method with spectral integration in the homogeneous direction. The high Pr was used to match the simulation with the conditions of the ongoing experimental project in our group using water (Verdoold et al., in preparation). The simulations require about 4000 h for one turnover time on one TERA processor, but with massive parallelisation on 192 processors this is reduced to less than a day (≈ 20 h) making it now possible to run the simulation over quite a few convective time scales. For this Ra number, one turnover time corresponds to about 55 s of real time of an experiment with water. The results, though still being processed (what is becoming a demanding and quite engaging task), have made possible to make some new and interesting deduction e.g. in regard to scaling and in defining for the first time the wind in a large aspect ratio domain with open ends (periodic boundary conditions) using a symmetry-accounting ensemble averaging (Van Reeuwijk et al., 2005). Figs. 4 and 5 show striking similarity of plume patterns detected experimentally by suspended liquid crystal (Fig. 4) and computed with DNS (Fig. 5), which can serve as mutual verification of two techniques. It is noted however, that the DNS data are much more comprehensive and permit to look at full time dynamics of the three-dimensional field, what is impossible by experiments. Fig. 6 shows a snapshot of the temperature field close to the bottom heated wall (at about $0.05\text{--}0.1H$, obtained by high-resolution DNS at $Ra = 10^8$! Bright yellow¹ colour indicates high temperature.

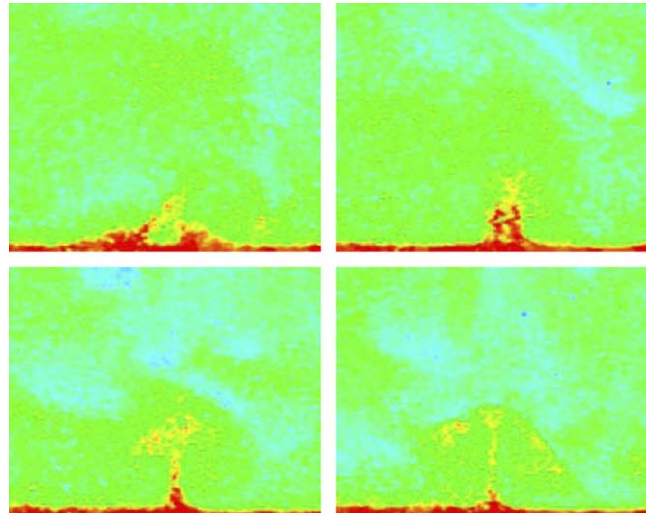


Fig. 4. Formation of a thermal plume in R–B convection, $Pr = 7$, $Ra = 10^8$. Visualization by suspended liquid crystals in a segment of the $4 \times 4 \times 1$ experiment with water (Verdoold et al., in preparation).

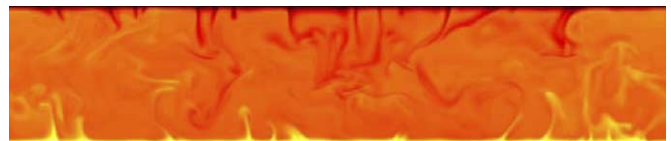


Fig. 5. A snapshot of DNS of temperature in the cross-section at the edge of $4 \times 4 \times 1$ periodic domain of R–B convection at $Ra = 10^8$, $Pr = 7$ (Van Reeuwijk, in preparation).

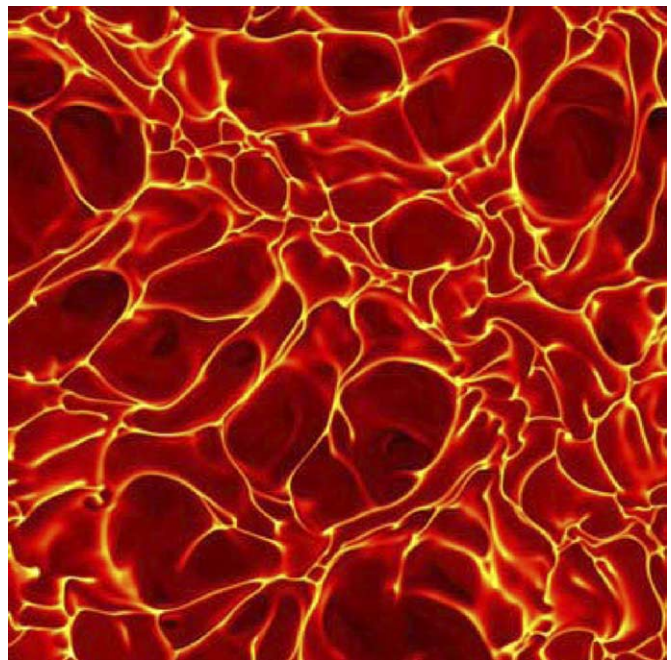


Fig. 6. A snapshot of DNS of temperature in a horizontal plane at $z = 0.05H$ in R–B convection at $Ra = 10^8$, $Pr = 7$, grid $768^2 \times 320$ (Van Reeuwijk, in preparation).

¹ For interpretation of colour in figures, the reader is referred to the Web version of this article.

The broad planform structures (indicating well established horizontal boundary layers) spoked by thin plume

sheets have been recorded earlier both in numerical simulations and in experiments, but not with such high resolution.

These new DNS results represent an important step forward in CS of R–B convection and will undoubtedly bring some valuable new information. But the severe limitation in the maximum attainable Ra number remains the major impediment. Large-eddy simulations may increase the limiting Ra number by one decade or so, but the crucial challenge remains in simulation of extreme Ra numbers of $O(Ra^{15}$ to $Ra^{20})$, which are at present also hardly accessible to experiments.

The only feasible way to reach such high Ra numbers is by statistical modelling either in the framework of one-point closures (URANS, T-RANS) or by coarse LES in which very large scales are resolved in time and space, but by modelling a much larger portion of the spectrum than practiced in the conventional LES. Such an approach, termed sometimes as VLES (very large eddy simulations) requires a RANS statistical or other type of models for the unresolved sub-scale motion, and especially for the near-wall region, thus leading towards merging the RANS and LES strategies.

An example of the T-RANS simulations, presented in terms of planform structure with spoke patterns in between (visualized by a surface of constant temperature coloured with the intensity of the vertical velocity) is shown in Fig. 7 for $Ra = 6.5 \times 10^5$ and $Ra = 2 \times 10^{13}$ (Kenjereš and Hanjalić, 2002). Comparison with DNS for the lower Ra number ($Ra = 6.5 \times 10^5$) shows that T-RANS reproduces the structure pattern in close resemblance with DNS (the latter with much finer grid), safe for very small structures, which remain ‘invisible’ to T-RANS. This comparison provides a verification of T-RANS and justification for its extrapolation to very high Ra numbers.

2.3. Synergy of experiments and simulations of R–B

After reviewing major limitations of experimental and simulation methods, we can summarize some interesting synergy outcomes from interactive experiments and simulations in R–B convection. The phenomenon of sudden or gradual reversal of flow direction illustrated in Figs. 2 and 3 awaits new computer simulations for further explanation, but it is also an incentive for CS. Whilst such records could easily be detected by CS by recording any of the observable properties at some monitoring points, as often is done in CS, the very long time scale of such events of 300–2000 s of real time, Figs. 2 and 3, would not be a probable outcome of a CS simply because it would require very long and expensive computation over dozens of turnover times, thus much longer than needed (and usual practiced) for gathering reliable statistics. However, the above and some other experimentally detected events will stimulate and make purposeful new much lengthier computations to provide clarification of these and perhaps some other phenomena.

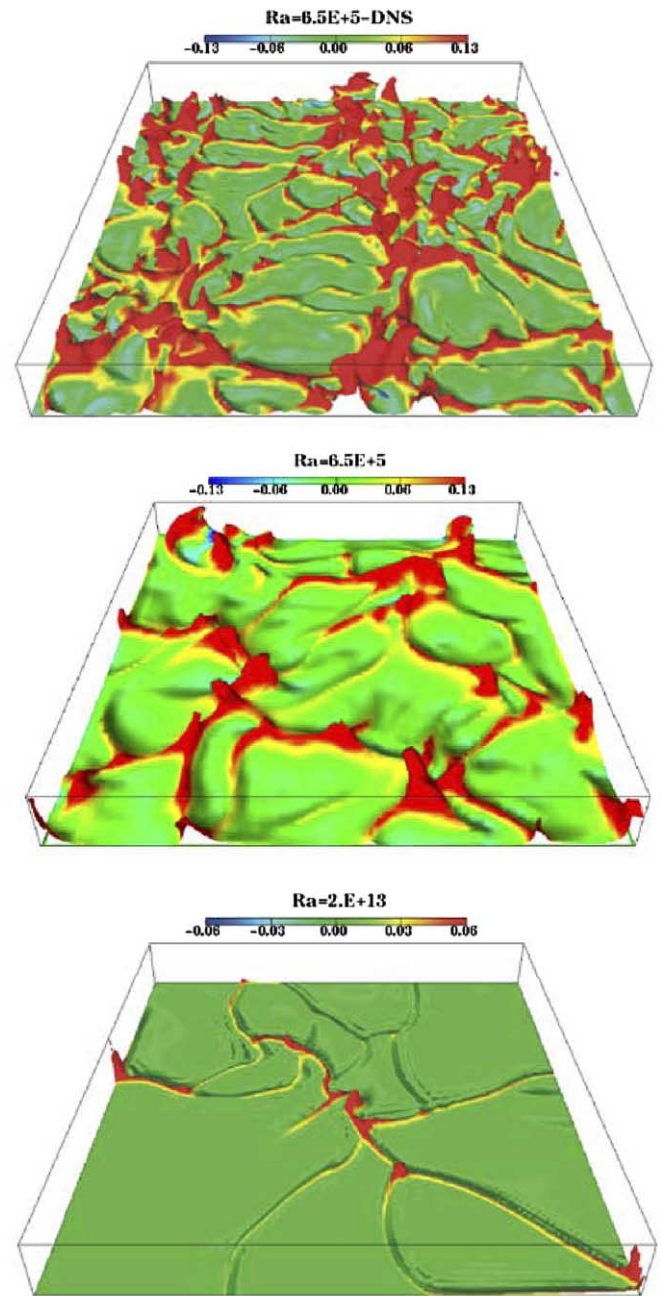


Fig. 7. DNS (top) and T-RANS (middle and bottom) computations of R–B for $Ra = 6.5 \times 10^5$ and 2×10^{13} , showing planform structures with plume sheets in between (Kenjereš and Hanjalić, 2002).

Another example of the synergy is the experimentally detected change of regime at Ra about 10^{12} , mentioned above. A selection of experimental and simulation results is shown in Fig. 8. Apart from results of Niemela (2000), most experiments and T-RANS simulations show a visible change of slope of the curve with the exponent of Ra changing from approximately 0.3 to significantly higher values. Transition at roughly the same Ra number are also visible in the thicknesses of the hydrodynamic and thermal boundary layers, λ_v and λ_θ respectively, which start to depart from the common scaling laws $\lambda_v/H \propto Ra^{-1/7}$ and $\lambda_\theta/H \propto Ra^{-1/3}$, Fig. 9.

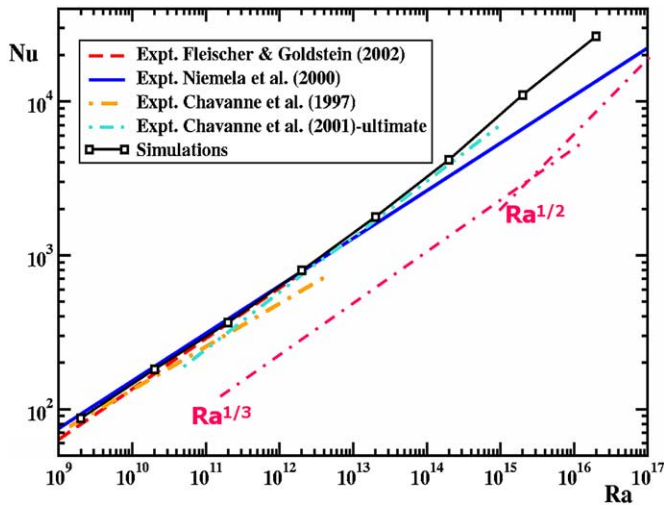


Fig. 8. A selection of experimental and computational results for Nusselt number versus Rayleigh number over 8 decades (Kenjereš and Hanjalić, 2002).

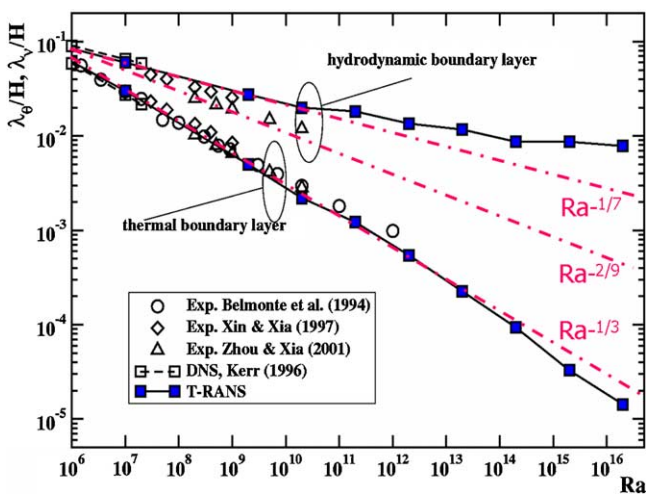


Fig. 9. Measured and computed hydrodynamic and thermal boundary layer thicknesses over 10 decades of Ra numbers (Kenjereš and Hanjalić, 2002).

While this transition may be formally linked with the asymptotic theory of Kraichnan (1962) for $Ra \rightarrow \infty$, its mechanism has never been fully clarified because of difficulties in experiments and impossibilities of DNS or LES at such high Ra numbers. This challenge has motivated us to use a VLES approach. It is interesting that the T-RANS reproduces a change of the regime as indicated in Figs. 8 and 9. Whilst this can be regarded as a very pleasing outcome, the question remains how much faith one should have in predicting a transitional event and its threshold with a CS that involve a semi-empirical RANS model as does the T-RANS (though calibrated in other generic flows, including by-pass transition in e.g. natural convection over a heated vertical plate). Here we need again some new, dedicated experiment!

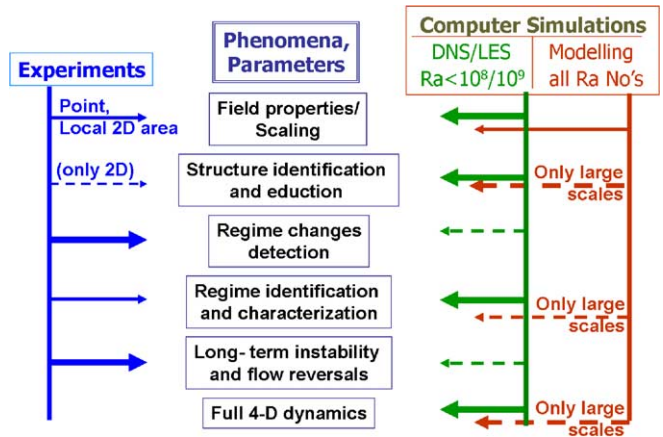


Fig. 10. Complementarity and synergy of experiments and computer simulations in R-B.

A comprehensive strategy, adopted in our group, consists of experiments ($Ra = 10^8-10^9$), DNS (10^5-10^8), LES (10^6-10^9) and VLES/T-RANS for $Ra = 10^6-2 \times 10^{16}$, conducted in parallel, with partial overlapping of Ra numbers, all aimed at complementary investigation that will provide mutual feedback and synergy. The potential of various research methods in providing information and in clarifying various events and phenomena is sketched in Fig. 10.

3. Impinging flows and heat transfer

Impinging jets from different orifices and in a variety of arrangements have been widely used for efficient heating and cooling of solid surfaces. While in most cases a significant heat transfer can be achieved, the optimum performance depends on a number of parameters, primarily on the shape of the jet-issuing orifice, its distance from the targeted solid wall, intensity and structure of turbulence in the jet and the overall configuration of the jet-surface assembly. With a single jet, very high heat transfer is achieved in the stagnation region, but further away from the stagnation point heat transfer rapidly decreases, resulting in large non-uniformity of the thermal field. Various modifications aimed at enhancing heat transfer have been investigated, such as jet inclination, swirl, forced—mechanical or acoustic—or self-induced excitation, special nozzle shapes. Most industrial applications involve multiple-jets in different arrangements, which lead to improved heat transfer uniformity, but bring into play additional parameters such as jet spacing (pitch), their relative positioning (in-line, staggered), and mutual orientation. In some cases, the jets are combined with a cross-flow and the target surface may not be stagnant. Also the impinging surface may not be flat nor smooth, but oblique and rough, or consisting of discrete objects such as in electronics cooling and in internal cooling of gas-turbine blades. Because of such a multitude of parameters that need be considered, optimal design of a jet arrangement can be quite a demanding task.

In addition to technological interest, impinging flows pose interesting challenge for studying physics of turbulence and heat transfer: a number of events and phenomena are encountered with rapid change of conditions, ranging from stagnation, jet deflection associated with strong acceleration, followed by development of a radial wall jet subjected to strong deceleration and radial spreading. The major heat transfer mechanism is believed to be associated with the surface renewal effects by large-scale eddies, originating from the break-up of toroidal vortices (in circular jets) formed in the mixing layer around the jet. Because of their inherent periodicity, the ring vortices cause alternating acceleration and deceleration of the jet's core, resulting in its pulsation with the natural frequency defined by jet velocity and orifice-to-plate distance. These pulsations weaken the boundary layer stability in the stagnation region affecting the heat transfer.

In multiple jets, additional phenomena appear such as jets interaction prior to impingement, collision of the wall jets, ejection fountains, recirculation and embedded vortices in the space between the jets, and unavoidable cross-flow towards the fluid escape openings. Recent PIV measurements and computer simulations indicated that in some cases (depending on jet spacing and orifice-plate distance), some jets never reach the target surface because of a strong cross-flow from neighbouring jets, thus diminishing the anticipated heat transfer enhancement, as shown in Fig. 11. All these events and complex flow structure leave thermal imprints on the target surface with possibly large non-uniformities in heat transfer.

Most studies of impinging jets and related heat transfer, have been experimental, focusing primarily on establishing heat transfer correlations in terms of mean flow properties and jets configuration, and to a lesser extent on measuring mean velocity and temperature in the fluid. Realizing that the essence of heat transfer enhancement lies in adequate control of flow and turbulence structures and their interaction with the impingement surface, recent investigations have focused more on studying the details of instantaneous flow and temperature fields and on establishing connections

and correlations between the eddy structure and the surface temperature or heat flux. The latter proved to be quite challenging especially at higher Re numbers. Capturing and measuring of the *instantaneous temperature field* and its turbulent fluctuations on a solid surface is still not readily tractable by any existing experimental technique. The frequency response of the currently available (expensive) fast infrared scanners is less than 100 Hz and is even less of the micro liquid crystals encapsulated in sheets or sprayed over a surface (Geers et al., 2004). These techniques can suffice only for experiments with water and some other liquids at low Re numbers. On the other hand, computer simulations (DNS, LES), which in principle could provide all information on instantaneous fields, are applicable only for low Re numbers. A combined and complementary approach seems not only beneficial, but also unavoidable.

We discuss two examples of synergy of experimental and computational investigations of impinging flows. The first is a single normally impinging round jet issuing from a long pipe (fully developed pipe flow) with orifice to plate distance $H = 2D$. For this configuration, at $Re > 15000$ experiments (Baughn and Shimizu, 1989) show that Nusselt number exhibits a second peak (next to one in the stagnation point), which becomes more pronounced as Re increases. This peak has been associated with high turbulence level in the shear layer at the jet edge, reaching the target plate. The phenomenon is obviously related to the shape of the orifice and its edges (whether sharp-edged or contoured) and to the turbulence level in the orifice and upstream from it. Controversy surrounds also the maximum Nu in the stagnation point, because the turbulence level here is relatively small and, according to some recent measurements and simulations, the production of the kinetic energy is here locally negative (though quite small), (Geers et al., 2004). Clarification of these and many other queries in regard to local heat transfer requires detailed insight into the flow and eddy structure. While these could in principle be gathered with tedious screening of the field with PIV, LDA or similar techniques (although the accuracy in the regions very close to the wall remains questionable),

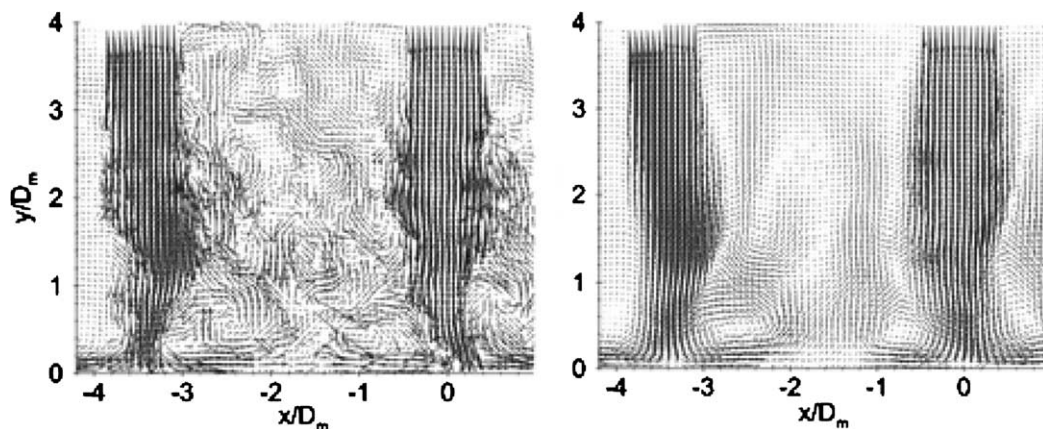


Fig. 11. PIV of multiple-impinging jets. Left original snapshot; right: POD filtered snapshot (Geers et al., 2005).

only CS could provide full three-dimensional fields with their time dynamics.

We performed LES of a single round impinging jet with $H/D = 2$ at $Re = 20000$ replicating the experimental set-up of Baughn and Shimizu (1989), and of Geers et al. (2004), aiming at complementing their results with information that are inaccessible to measurements (Hadžiabdić and Hanjalić, in preparation). The task took more effort and time than anticipated: with an adaptable unstructured grid, several grid refinements have been performed to meet the grid resolution requirements. The criteria used were based on the estimated Kolmogorov scale (using RANS computations) as well as those established for equilibrium wall-attached flows ($\Delta y^+ < 1$, $\Delta z^+ < 20$, $\Delta x^+ < 50$). The simulations were eventually performed with 10 million grid cells for the complete jet and with 5 million for one quadrant using periodic boundary conditions, the latter being equivalent to 20 million for the complete jet. Yet, the results for the Nu number are still not in full accord with measurements, as shown in Fig. 12, especially for $r/D > 2.5$ where the computational grid begins rapidly to depart from the above defined criteria.

This indicates that capturing the specific phenomena, such as wall friction and temperature especially around the second Nu peak around $r/D = 2$, where the boundary layer is very thin and undergoes a transition from strong acceleration due to jet deflection to strong deceleration due to radial spreading, is very demanding on grid resolution. It should be noted that the inflow conditions were generated by an a priori LES of a fully developed pipe flow to replicate closely the experiments, though, admittedly, the pipe wall thickness (3 mm at $D = 50$ mm) has not been accounted for in LES. For curiosity, we mention that RANS computation with an elliptic-relaxation

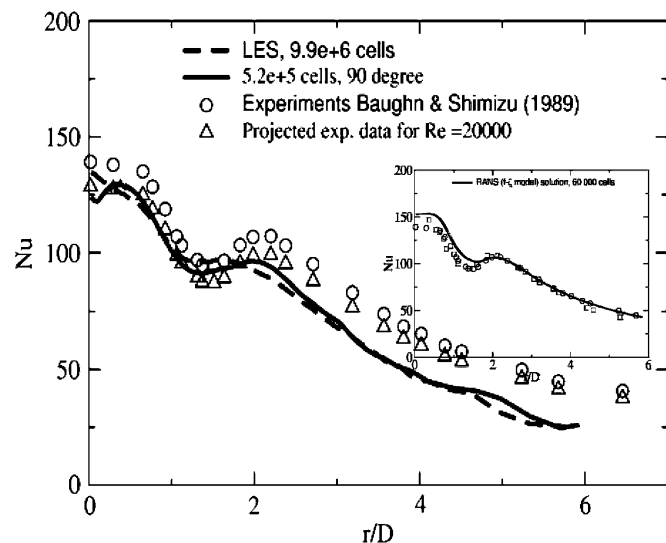


Fig. 12. Limitations of LES in impinging flows at higher Re numbers: LES with 10 and 20 million cells still insufficient for $Re = 20000$ (Hadžiabdić and Hanjalić, in preparation). Insert: RANS with 80000 cells (Hanjalić et al., 2004).

eddy-viscosity model (ζ - f , Hanjalić et al., 2004) with only 80000 grid points shows excellent agreement with experiments.

The second example is a cluster of multiple (9) jets. We performed experiments and RANS computations with different models of two different (in line and hexagonal) arrangement, with a sharp-edge and contoured nozzles, all at $Re \approx 20000$. The PIV, LDA and liquid crystals sprayed over the heated impinged surface were processed in various ways, including proper-orthogonal decomposition, revealing a number of interesting phenomena, especially on the interaction and collision of neighbouring jets, as already mentioned and shown in Fig. 11 (Geers et al., 2005).

We focus here only on some features that illustrate synergy effects. One of the most interesting events was detected by RANS computations: in the in-line configuration, the resulting steady solutions showed visible asymmetry around the 45° axis, despite the imposed symmetry conditions in the geometry (a quadrant of the complete field) and boundary conditions. Instead, an embedded weak vortex was detected in the upper side close to the projection of the central orifice, indicating a deflection of the central jet towards the upper left jet, Fig. 13. The phenomenon, although with somewhat different intensity, was detected with three different turbulence models: the standard k - ϵ with wall functions, v_2 - f elliptic-relaxation eddy-viscosity model, and the elliptic-blending second-moment (Re stress) closure, the latter two involving integration up to the wall (Thielen et al., 2005).

Admittedly, because of their inherent empiricism (modelling is in essence an approximation), the RANS computations have never been regarded as a true and reliable research instrument, but rather as an engineering “extrapolation” tool with limited predicting capabilities. Hardly anyone would believe claims in discovery of a physical phenomenon by RANS. Our first reaction was of that nature, suspecting a computational artefact due to a bug in the numerical code! However, careful checking and repetition of computations (steady and unsteady) with different initial fields persistently repeated the event, though in some cases appearing mirrored on the other side of the 45° symmetry line. Fortunately, the experiments in the same project were still going on, and PIV measurements undertaken in several planes parallel to the wall conformed without any doubt that the event is not an artefact, but a true physical phenomenon. Once we were confident that the event is real, a plausible explanation was related to physical system asymmetry and possible local bifurcation pertinent to this particular (in-line) orifice configuration: a low momentum vortex is created and trapped in the inter-jet space either on one or the other side of the symmetry plane.

Of course, this asymmetric flow pattern leaves an asymmetric thermal imprint on the target surface, which was captured by all RANS models used, though with different quality, as shown in Fig. 14. (For details see Thielen et al., 2003).

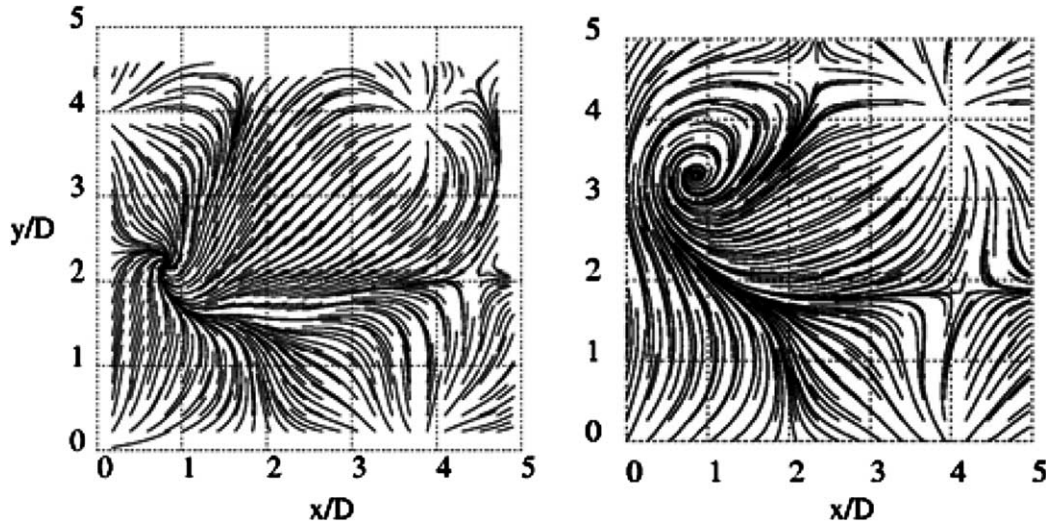


Fig. 13. Asymmetric pathlines at $0.54D$ above the impingement plate in a quadrant of multiple jets with in-line symmetric arrangement. Left: PIV measurements; right: computations, RANS v2-f model (Thielen et al., 2003).

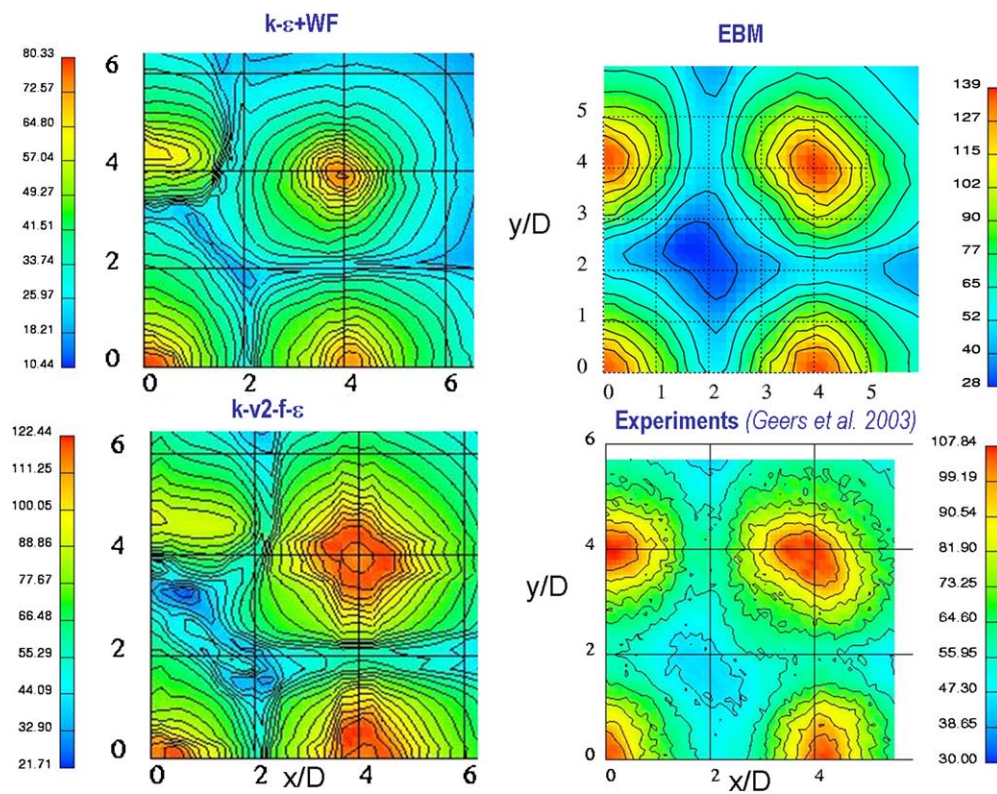


Fig. 14. RANS computations and Liquid Crystal measurements of Nusselt number on the impingement surface in an in-line multiple jets arrangement. Top left: $k-\epsilon + WF$, top right: EBM, bottom left: v2-f (Thielen et al., 2005); bottom right: LCT measurements (Geers et al., 2004).

The event itself may not be of great importance (though its thermal imprint shows significant effect on the uniformity of the heat transfer), but has been merely introduced here as an illustration of synergy between experiments and computations. It may sound strange to some that a physical event or phenomenon was first detected by RANS com-

putations, which first triggered a new experimental lookup to provide a verification, but expanded later into more detailed experimental studies of the vortical structure in the multiple impinging jets, and its correlation with the thermal field and heat transfer on the impinging surface (Geers et al., in press).

3.1. Fluid magnetic dynamo

The fluid-magnetic dynamo (popularly known also as hydromagnetic dynamo) is believed to be the origin of all magnetic fields in nature and the basic mechanism of their self-excitation and sustenance in Earth and most other celestial bodies. The notion implies the generation of a magnetic field in moving electro-conducting fluids, such as liquid metallic core of the Earth that moves by thermal convection from its interior out to the mantle, and due to Earth rotation. This motion through the already existing magnetic field induces electrical current within the core (“dynamo”). The magnetic field associated with these currents amplifies the original field, ensuring that it does not decay with time. The process goes at the expense of Earth internal energy. A weak interplanetary magnetic field could have provided the original source field for this process (Jackson, 2000).

A plausible model, underlined with elaborate theory, was established in early twenties of the last century, but was not proved until 1999, when the long and enduring experiments in Riga (Latvia) and soon afterwards in Karlsruhe (Germany) succeeded in creating right conditions in which an enclosed moving fluid can amplify and maintain a magnetic field starting from the weak background field. Fig. 15 shows a recording of the magnetic field self-excitation and the achieved saturation level at one measuring point in the experimental rig (Fig. 16) during one of many experimental campaigns in Riga. The diagram shows

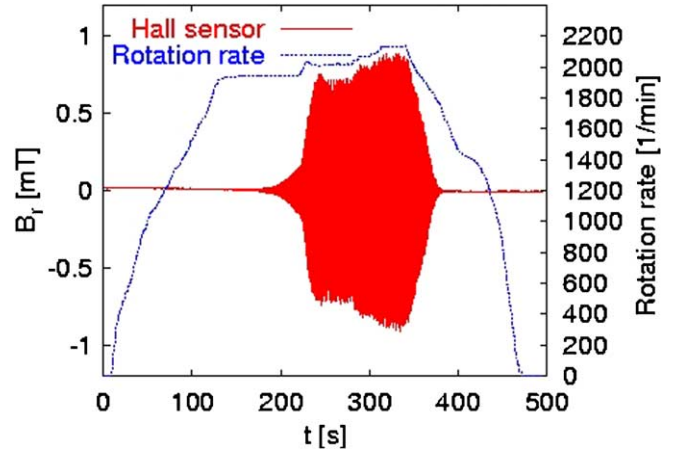


Fig. 15. A recording of the magnetic field self-excitation and saturation in one of the experiments in Riga, with indicated rotation speed of the swirler (Gailitis et al., 2002).

also the rotation rate of the swirler that generates a strong swirling of the inflowing fluid.

The geometries and flow patterns in the Riga and Karlsruhe experiments are quite different among themselves but also from that in Earth, but what matters is the proper constellation of the rig’s dimension, fluid velocity and direction, and the fluid properties. To achieve right condition in a laboratory required a lot of ingenuity and overcoming enormous technical difficulties. The main obstacle to a successful experimental replication is the requirement

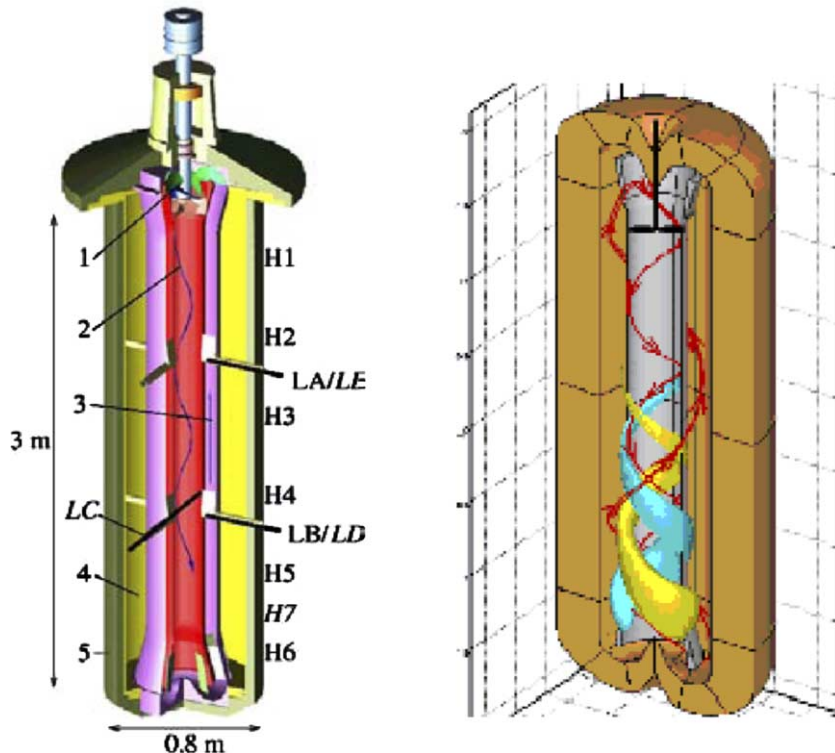


Fig. 16. Schematics of Riga experiment with indicated dimensions and position of Hall sensors (left) and a view of computer simulation of the magnetic field, with a frozen velocity field (right) (Kenjereš et al., in preparation).

to achieve the critical magnetic Reynolds number, which requires large-scale apparatus with high velocity of the moving fluid. The self-excitation of the magnetic field is similar to laminar-to-turbulent transition and occurs when the magnetic Reynolds number $Rm = LU/\eta$ exceeds the critical value, which—depending on the flow pattern and geometry—is in the range of 10 – 10^3 (here L and U are the characteristic length and velocity scales, just as in the hydrodynamic Re numbers, and $\eta = 1/\mu\sigma$ is the magnetic diffusivity of the fluid, μ is the magnetic permeability and σ electric conductivity). Because even in best liquid electrical conductors (e.g. sodium) $\eta \geq 0.1$ m²/s, the product of velocity and length scale should be of the order of 1 – 10 m²/s, which is not easy to achieve in experiments with electrically conductive fluids. It is noted that for such length–velocity products, the hydrodynamic Re number is very high—for typical electro-conductive fluids of the order of 10^6 , or higher, implying highly turbulent flow regimes.

It is beyond the scope of this article to go into all intricacies of magnetic dynamos (for more details see e.g. Gailitis et al., 2002; Gailitis et al., 2001; Jackson, 2000). We have selected this example partly because we have been involved in attempts to complement this experiment with computer simulations, but more because this problem is in our view an excellent example of synergy of theory, experiments and computer simulations. From the advent of computers, numerical simulations have been used for studies of hydromagnetic dynamos, but using highly simplified models far from mimicking real situations. Because of the nature of the phenomenon, which is in essence a bifurcation transition, just as in other cases of transitions from one regime to another, no computational proof of the phenomenon nor of the threshold criteria for its occurrence would be acceptable as sufficient proof because of inherent uncertainties in numerical accuracy associated with unknown phenomena. The limitations to simulations are of the same nature, but even more severe than in experiments: simulating the self-excitation (kinematics) and the maintenance of the magnetic field (saturation regime) requires essentially direct numerical simulation (DNS) of the *magnetic induction equation*, coupled with some advanced simulation method that can capture reasonably well at least the large structures of the velocity field and turbulence that are interacting with the unsteady magnetic field. In his enlightening article on the success of Riga and Karlsruhe experiments, Jackson (2000) wrote that “... these two experiments operate in a regime that so far has been inaccessible to numerical simulations”, but closes with an optimistic statement that “experimental dynamos have emerged at the same time that large numerical simulations have reached some maturity”. This statement can be interpreted as a challenge and a synergic incentive to computer simulations. We can expand this by adding that because the DNS of the *velocity* field for such high Re numbers are far beyond the reach of present computers, coarse LES or VLES (hybrid RANS/LES) that are currently being developed worldwide among computational communities,

seem the only viable way to handle the velocity field, coupled with DNS of the magnetic induction equation. Such an approach is currently underway at Delft University of Technology, and very recently we succeeded in reproducing computationally the findings of the Riga experiment!

Several decades of research on Riga experiment involving theory, experiments and simulations, have already demonstrated great benefits of synergy from using complementary research methods. It is recalled that in order to achieve right conditions (length–velocity product) for the magnetic field self-excitation, all experiments attempted in the past, involved complex flow passages with rotation and swirl. The Riga experiment was envisaged as a strong swirling motion of liquid sodium, generated by a swirl generator driven by a powerful electromotor (240 KW), Fig. 16. The Riga experiment, just as all others, was not intended to model any of the celestial bodies, but to demonstrate the basic dynamo mechanism, i.e. that the intense motion in a large volume of a good electro-conducting liquid creates a magnetic field. The design of the experimental rig was preceded by optimisation studies involving costs and technical realisability, complemented with preliminary experiments in a down-scaled model with water and computer analysis of the swirler design using a commercial CFD code with the standard RANS turbulence model. These computations were subsequently replaced by more reliable ones using our in-house CFD code and more advanced turbulence models. The aim was to find the inflow velocity profile, appropriate for achieving the critical magnetic Re number, but requiring minimum pumping power. For such tasks, the CFD modelling appeared to be invaluable, despite some uncertainties in the accuracy of RANS models.

The experimental replication of the magnetic self-excitation was the main target of all experiments, but with its success the mission is still not fully accomplished. It is noted that in all experiments, non-transparent liquid metals are used as fluids, and in some cases under pressure and higher temperature thus severely restricting measurements of any flow properties. Apart from some point measurements of the intensity of the magnetic field, no information is available about fluid velocity and temperature, let alone turbulence. While all these parameters may be considered of secondary importance once the experiment was successful, the research of the phenomenon of magnetic dynamo in Earth and celestial systems would greatly benefit from such information. This is where the computer simulations are the only hope and where the synergy will be the greatest.

As an illustration, we show some results of computer simulations of the Riga experiment. In the first case (“one-way coupling”), the velocity and magnetic fields are decoupled. First the velocity field has been computed using an advanced RANS turbulence model, thus generating a steady velocity field and basic turbulence statistics (second moments). An a priori obtained approximate magnetic field was fed into computations to account for its

effect on the velocity field and turbulence statistics through the mean Lorentz force. Then these results are fed into the magnetic induction equation, which is solved numerically in time and space. The numerical mesh and especially the time steps are sufficiently fine to regard these solution as *direct numerical simulation* of the magnetic field B (DNS-B). Note that the self-excitation of the magnetic field is sinusoidal with expected frequency of $O(1-10)$ Hz, so the DNS of the induction equation, safe for its instantaneous interaction with the turbulence fluctuations, is not as great challenge as the DNS of the velocity field. Here we simulate only the so called kinematic regime: the development of instabilities and self-excitation of the magnetic field, but no interactive feed back of magnetic field into the velocity field, Fig. 17. The simulation of the kinematic regime (denoted by a circle in Fig. 17 left) for a range of Re_m (20–50) and $Re = 3 \times 10^6$ brought already valuable information on the effects of the imposed magnetic Re number on the frequency of the self-excitation signal.

The real aim and challenge is, however, the simulation of the full “two-way” coupling in so called “saturation regime”, recorded in the experiment, in which the generated magnetic field feeds back and attenuates the magnetic oscillation to the level corresponding to the balance of the Lorentz and inertial forces, but also excites the velocity field (in the kinematic regime assumed to be steady). This two-way coupling has been tested successfully in some simpler, generic, test cases. The full “two-way” simulations reproduced very realistic excitation and subsequent saturation of the magnetic field with frequencies and amplitudes in

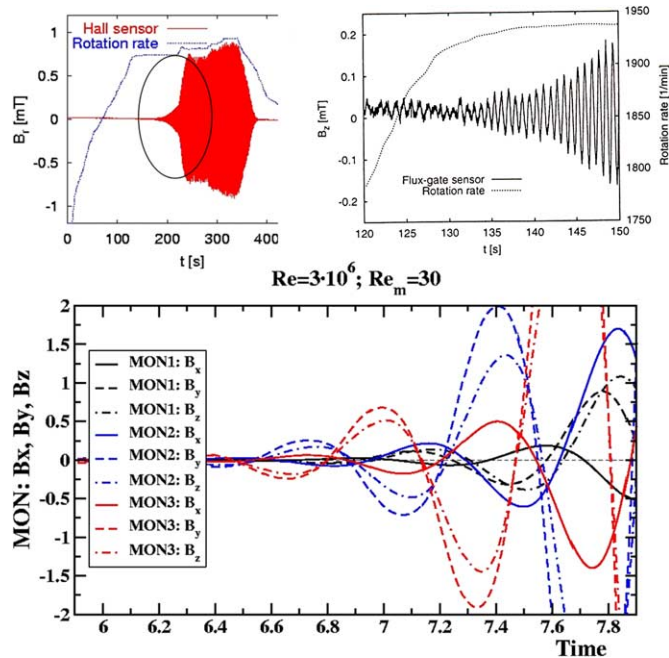


Fig. 17. Computer simulation of the self-excitation of the magnetic field (right); lines indicate different monitoring locations (Kenjereš et al., in preparation). Left: experiments—a blow up of the kinematic regime (encircled) in the experimental recording (Gailitis et al., 2002; Gailitis et al., 2001).

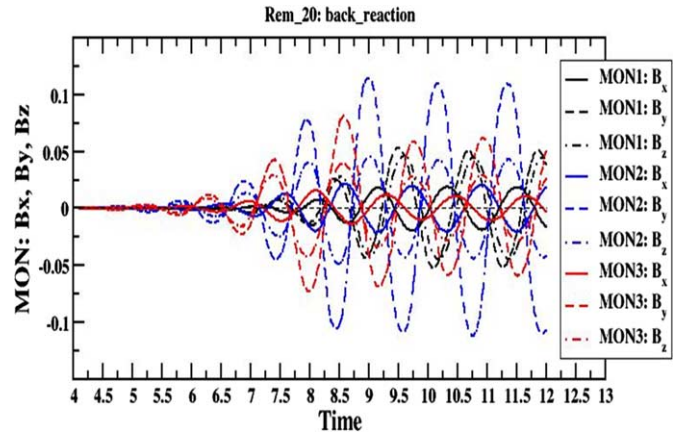


Fig. 18. Computer simulations of the two-way coupling (saturated regime) of the Riga experiment; lines indicate different monitoring locations (Kenjereš et al., in preparation).

full accord with Riga experimental finding, as illustrated in Fig. 18 by histograms of all three components of the magnetic field at several monitoring points.

But perhaps the most valuable outcome of such simulations is the computer visualization of the complex velocity and magnetic fields and their interaction. Fig. 19 shows some results of a snapshot of the magnetic field for

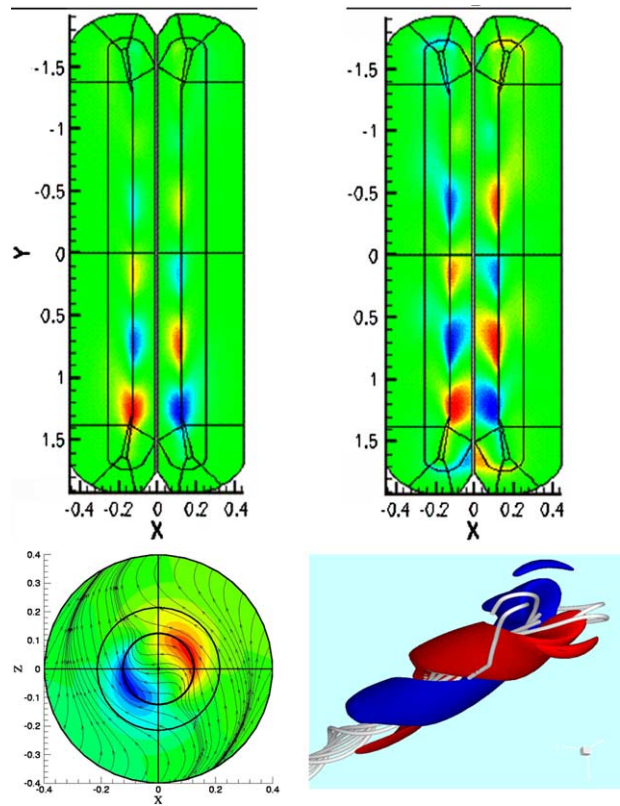


Fig. 19. Computer simulations of the magnetic field self-excitation in a model of Riga experiment. Top: axial and tangential magnetic field components. Bottom left: magnetic field in a cross-section with indicated magnetic lines. Bottom right: a 3D snapshot of the magnetic field with fluid pathlines in the background (Kenjereš et al., in preparation).

$Re_m = 30$, just as an illustration of the CS capturing of the self-excitations in the kinematic regime. A 3D view of the velocity and magnetic field is shown in Fig. 19 below right.

4. Conclusions

Potential and benefits of synergy of experiments and computer simulations in turbulent convection have been discussed by way of three examples of turbulent convection, currently under investigation in the author's group. The examples considered are the thermal convection over horizontal heated surfaces, but at a range of conditions and regimes including extreme Rayleigh numbers; flow and heat convection in single and multiple jets impinging on a solid surface, and magneto-fluiddynamic problem related to fluid dynamos. Each of the cases poses some new challenges—events or phenomena—that have been discovered or detected by either experiment or simulations, but requiring other method to complement the research and to provide additional information for event clarification. Each of the flows considered involves some changes in regimes and consequent changes of scaling.

All three classes of problems here considered have long been investigated both experimentally and by computer simulations. We reviewed briefly limitations of each technique in specific problems and indicated beneficial synergy effect when both, experiments and computer simulations are used in parallel in a systematic manner. Some conclusions that emerged, although not meant to be general, can be summarized in the following:

- The robustness and repeatability of most experimental techniques will keep experiments irreplaceable in detecting new physical events and phenomena, in gathering basic information in new configurations, set-ups and conditions, as well as for verification of any new events detected by computer simulations. The experiments will also remain the basic instrument for validating and calibrating of any mathematical model of a physical phenomena or processes. New non-intrusive optical techniques have already boosted experiments' capabilities to gain space and time field data, and these can be expected to advance. Though, full and well resolved time dynamics of the complete 3D fields will remain for long beyond the reach of experimental techniques.
- Computer simulations, on the other hand have emerged as an indispensable tool for collecting detailed high-resolution 3D information in space and time. Especially the DNS and fine-LES are regarded now as the true research methods that can provide, in principle, answers to just about any question. But the limitations in regard to grid density, although expected to relax gradually with time, will keep some interesting and challenging phenomena pertinent to very high Re and Ra numbers beyond the reach of DNS and LES. Within the range of indubitable faithfulness, because of expenses and time, DNS will remain primarily useful in gaining deeper insights into problems that have already been investigated and detected, and this will remain the major synergy benefit. But the potential of DNS and LES for discovering new physics, could be increased in closer interaction with experiments, by e.g. following hints from experiments to define the focus of investigation and then performing systematic and sufficiently long simulations with consistently reliable accuracy over a broad range of conditions, what has not been the practice so far.
- Semi-empirical and mixed approaches such as URANS, VLES, hybrid RANS/LES, will serve for tackling problems that are beyond the reach of DNS and LES and provide useful information complementing experiments. But, because of their (semi)empirical flavour, they will hardly ever be accepted as trustful and robust (in the sense of repeatability) research instrument when it comes to detecting and discovering of new physics. And this includes various changes of regimes and transitional phenomena. Nevertheless, these methods will remain for long irreplaceable and extremely useful complementary tools, and in combination with experiments, will generate much synergy.
- Computer visualization and animation, while pioneered in experimental research, have reached their full blossom with the computer simulations thanks primarily to the abundance of high-resolution data generated by CS. The CS results can be processed, filtered, visualized and animated, looked from different angles and viewpoints, and can reveal events, phenomena, structures, which may be just too complex for abstract imaging in ones mind. In many examples, only a genius mind could have thought of and visualize in his mind what is now accessible by computer visualization to anybody. Computer visualization is growing into its own branch of science.
- But, with all these developments, progress and prospects some new problems are becoming increasingly acute: tremendous amount of data generated, especially with CS. As G. Ehrenman wrote recently (Ehrenman, 2005) "Having terabytes of data at our disposal greatly increases the chances that you will find the answer to even the toughest questions – if you don't mind searching for a needle in a giant digital haystack". We add here that a good hint for where to look can come from experiments, and that would already be a valuable synergy.

Acknowledgements

I thank my colleagues and students L. Geers, M. Hadžiabdić, H. Jonker, S. Kanjereš, M. van Reeuwijk, L. Thiesen, M. Tummers, J. Verdoold for their input and fruitful discussion.

References

- Baughn, J.W., Shimizu, S., 1989. Heat transfer measurements from a surface with uniform heat flux and an impinging jet. *Trans. ASME—J. Heat Transfer* 111, 1096–1098.
- Castaing, B., Gunaratne, G., Heslot, F., Kadanoff, L., Libchaber, A., Thomae, S., Wu, Z.X., Zaleski, S., Zanetti, G., 1989. Scaling of hard thermal turbulence in Rayleigh–Bénard convection. *J. Fluid Mech.* 204, 1–30.
- Chavanne, X., Chilla, F., Castaing, B., Hébral, B., Chabaud, B., Chaussy, J., 1997. *Phys. Rev. Lett.* 79, 3648.
- Chavanne, X., Chilla, F., Chabaud, B., Castaing, B., Hébral, B., 2001. Turbulent Rayleigh–Bénard convection in gaseous and liquid He. *Phys. Fluids* 13 (5), 1300.
- Ehrenman, G., 2005. Mining what others miss. *Mech. Eng. (ASME)* 127/2, 26–31.
- Gailitis, A., Lielausis, O., Platacis, E., Dementev, S., Ciferons, A., Gerbeth, G., Gundrum, T., Stefani, F., 2001. Magnetic field saturation in the Riga dynamo experiment. *Phys. Rev. Lett.* 86, 3024–3027.
- Gailitis, A., Lielausis, O., Platacis, E., Gerbeth, G., Stefani, F., 2002. Laboratory experiments on hydromagnetic dynamos. *Rev. Mod. Phys.* 74, 973–990.
- Geers, L., Tummers, M., Hanjalić, K., 2004. Experimental investigations of impinging jet arrays. *Exp. Fluids* 36, 946–958.
- Geers, L., Tummers, M., Hanjalić, K., 2005. PIV-based identification of coherent structures in normally impinging multiple jets. *Phys. Fluids* 17(5), 055105:1–13.
- Geers, L., Hanjalić, K., Tummers, M., in press. Wall imprints of turbulent structure and heat transfer in multiple impinging jet arrays. *J. Fluid Mech.*
- Glazier, J.A., Segawa, T., Naert, A., Sano, M., 1999. *Nature (London)* 398, 307–308.
- Hadziabdić, M., Hanjalić, K., in preparation.
- Hanjalić, K., Popovac, M., Hadziabdić, M., 2004. A robust near-wall elliptic-relaxation eddy-viscosity turbulence model for CFD. *Int. J. Heat Fluid Flow* 25, 1047–1051.
- Jackson, A., 2000. Critical time for fluid dynamos. *Nature* 405, 1003–1004.
- Kenjereš, S., Hanjalić, K., 2002. Numerical insight into flow structure in ultraturbulent thermal convection. *Phys. Rev. E* 66, 036307(1)–036307(5).
- Kenjereš, S., Hanjalić, K., Renaudier, S., Stefani, F., in preparation.
- Kerr, D., 1996. Heat transport in convection and the asymptotic state. *J. Fluid Mech.* 310, 139–179.
- Kraichnan, R.H., 1962. Turbulent thermal convection at arbitrary Prandtl number. *Phys. Fluids* 5, 1374–1389.
- Niemela, J.J., Skrbek, L., Sreenivasan, K.R., Donnelly, J.R., 2000. *Nature (London)* 404, 837–838.
- Niemela, J.J., Skrbek, L., Sreenivasan, K.R., Donnelly, R.J., 2001. The wind in confined thermal convection. *J. Fluid Mech.* 449, 169–178.
- Roche, P.E., Castaing, B., Chabaud, B., Hébral, B., 2001. Observation of the $a/2$ power law in Rayleigh–Bénard convection. *Phys. Rev. E* 63, 045303(R).
- Siggia, E.D., 1994. High Rayleigh number convection. *Annu. Rev. Fluid Mech.* 26, 137–168.
- Thielen, L., Hanjalić, K., Jonker, H.J.J., Manceau, R., 2005. Predictions of flow and heat transfer in multiple impinging jets with an elliptic-blending second-moment closure. *Int. J. Heat Mass Transfer* 48, 1583–1598.
- Thielen, L., Jonker, H.J.J., Hanjalić, K., 2003. Symmetry breaking of flow and heat transfer in multiple impinging jets. *Int. J. Heat Fluid Flow* 24, 444–453.
- Tummers, M.J., van Veen, E.H., George, N., Rodink, R., Hanjalić, K., 2004. Measurement of velocity–temperature correlation in a turbulent diffusion flame. *Exp. Fluids* 37, 364–374.
- Van Reeuwijk, M., Jonker, H.J.J., Hanjalić, K., in preparation.
- Van Reeuwijk, M., Jonker, H.J.J., Hanjalić, K., 2005. Identification of wind in Rayleigh–Bénard convection. *Phys. Fluids* 17, 051704:1–4.
- Verdoold, J., Tummers, M., Hanjalić, K., in preparation.
- Wu, X.-Zh., Kadanoff, L., Libchaber, A., Sano, M., 1990. Frequency power spectrum of temperature fluctuations on free convection. *Phys. Rev. Lett.* 64/18, 2140–2143.